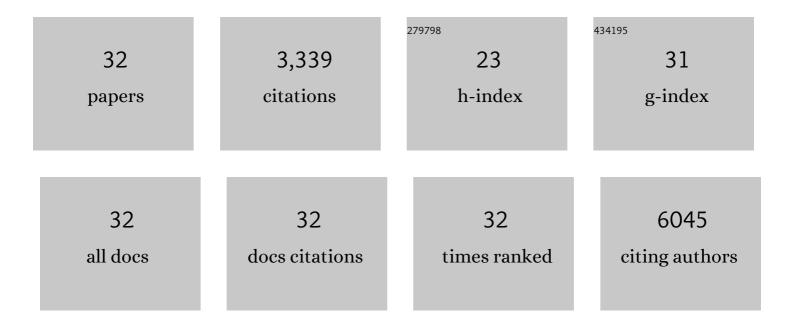
Matthew R Field

List of Publications by Year in descending order

Source: https://exaly.com/author-pdf/12097659/publications.pdf Version: 2024-02-01



#	Article	IF	CITATIONS
1	Metal–Organic Charge Transfer Complexes of Pb(TCNQ) 2 and Pb(TCNQF 4) 2 as New Catalysts for Electron Transfer Reactions. Advanced Materials Interfaces, 2020, 7, 2001111.	3.7	8
2	Long-range ordered TiO ₂ /Au hollow urchins: topology control for maskless electrodeposition. Journal of Materials Chemistry A, 2020, 8, 26035-26044.	10.3	8
3	Zinc Titanate Nanoarrays with Superior Optoelectrochemical Properties for Chemical Sensing. ACS Applied Materials & Interfaces, 2019, 11, 29255-29267.	8.0	23
4	Antisymmetric magnetoresistance in van der Waals Fe ₃ GeTe ₂ /graphite/Fe ₃ GeTe ₂ trilayer heterostructures. Science Advances, 2019, 5, eaaw0409.	10.3	119
5	Hard magnetic properties in nanoflake van der Waals Fe3GeTe2. Nature Communications, 2018, 9, 1554.	12.8	272
6	Broadband light active MTCNQ-based metal–organic semiconducting hybrids for enhanced redox catalysis. Applied Materials Today, 2018, 13, 107-115.	4.3	16
7	Defining the role of humidity in the ambient degradation of few-layer black phosphorus. 2D Materials, 2017, 4, 015025.	4.4	110
8	Degradation of black phosphorus is contingent on UV–blue light exposure. Npj 2D Materials and Applications, 2017, 1, .	7.9	95
9	Highâ€Performance Field Effect Transistors Using Electronic Inks of 2D Molybdenum Oxide Nanoflakes. Advanced Functional Materials, 2016, 26, 91-100.	14.9	164
10	Candle-Soot Derived Photoactive and Superamphiphobic Fractal Titania Electrode. Chemistry of Materials, 2016, 28, 7919-7927.	6.7	36
11	Robust Nanostructured Silver and Copper Fabrics with Localized Surface Plasmon Resonance Property for Effective Visible Light Induced Reductive Catalysis. Advanced Materials Interfaces, 2016, 3, 1500632.	3.7	46
12	Exfoliation Solvent Dependent Plasmon Resonances in Two-Dimensional Sub-Stoichiometric Molybdenum Oxide Nanoflakes. ACS Applied Materials & Interfaces, 2016, 8, 3482-3493.	8.0	111
13	Enhanced Gas Permeation through Graphene Nanocomposites. Journal of Physical Chemistry C, 2015, 119, 13700-13712.	3.1	70
14	Self-assembled V2O5 interconnected microspheres produced in a fish-water electrolyte medium as a high-performance lithium-ion-battery cathode. Nano Research, 2015, 8, 3591-3603.	10.4	27
15	Supplementing Cold Plasma with Heat Enables Doping and Nanoâ€Structuring of Metal Oxides. Plasma Processes and Polymers, 2014, 11, 897-902.	3.0	1
16	Back Cover: Plasma Process. Polym. 9â^•2014. Plasma Processes and Polymers, 2014, 11, 904-904.	3.0	0
17	Two dimensional α-MoO3 nanoflakes obtained using solvent-assisted grinding and sonication method: Application for H2 gas sensing. Sensors and Actuators B: Chemical, 2014, 192, 196-204.	7.8	190
18	Exploiting the Facile Oxidation of Evaporated Gold Films to Drive Electroless Silver Deposition for the Creation of Bimetallic Au/Ag Surfaces. ChemElectroChem, 2014, 1, 76-82.	3.4	13

MATTHEW R FIELD

#	Article	IF	CITATIONS
19	Tunable Plasmon Resonances in Twoâ€Dimensional Molybdenum Oxide Nanoflakes. Advanced Materials, 2014, 26, 3931-3937.	21.0	308
20	Electrospun Granular Hollow SnO ₂ Nanofibers Hydrogen Gas Sensors Operating at Low Temperatures. Journal of Physical Chemistry C, 2014, 118, 3129-3139.	3.1	166
21	Substoichiometric two-dimensional molybdenum oxide flakes: a plasmonic gas sensing platform. Nanoscale, 2014, 6, 12780-12791.	5.6	77
22	A vein-like nanoporous network of Nb2O5 with a higher lithium intercalation discharge cut-off voltage. Journal of Materials Chemistry A, 2013, 1, 11019.	10.3	77
23	Electrochemical Control of Photoluminescence in Two-Dimensional MoS ₂ Nanoflakes. ACS Nano, 2013, 7, 10083-10093.	14.6	282
24	Electrochromic properties of TiO2 nanotubes coated with electrodeposited MoO3. Nanoscale, 2013, 5, 10353.	5.6	61
25	Nanoporous Nb2O5 hydrogen gas sensor. Sensors and Actuators B: Chemical, 2013, 176, 149-156.	7.8	123
26	Anodic formation of a thick three-dimensional nanoporous WO3 film and its photocatalytic property. Electrochemistry Communications, 2013, 27, 128-132.	4.7	58
27	Aqueous phase synthesis of copper nanoparticles: a link between heavy metal resistance and nanoparticle synthesis ability in bacterial systems. Nanoscale, 2013, 5, 2300-2306.	5.6	158
28	Enhanced Charge Carrier Mobility in Twoâ€Dimensional High Dielectric Molybdenum Oxide. Advanced Materials, 2013, 25, 109-114.	21.0	355
29	Enhanced Charge Carrier Mobility in Twoâ€Ðimensional High Dielectric Molybdenum Oxide (Adv. Mater.) Tj ETQq	1 1 0 7843 21.0	31 ₉ 4 rgBT /○
30	The anodized crystalline WO3 nanoporous network with enhanced electrochromic properties. Nanoscale, 2012, 4, 5980.	5.6	164
31	Elevated Temperature Anodized Nb ₂ O ₅ : A Photoanode Material with Exceptionally Large Photoconversion Efficiencies. ACS Nano, 2012, 6, 4045-4053.	14.6	174
32	Fabrication, Structural Characterization and Testing of a Nanostructured Tin Oxide Gas Sensor. IEEE Sensors Journal, 2009, 9, 563-568.	4.7	18